

<https://doi.org/10.48047/AFJBS.7.7.2025.6660-6689>



African Journal of Biological Sciences

Journal homepage: <http://www.afjbs.com>



Research Paper

Open Access

**Phenotypic and molecular characterization of *Myxobolus moliwensis* sp. nov. (Cnidaria: Myxosporea), a parasite of *Labeobarbus habereri* (Steindachner, 1914) from the Moliwè River in Limbé, Cameroon**  
**TCHOUTEZO-TIWA Amandine Estelle<sup>1\*</sup>, LEKEUFACK-FOLEFACK Guy Benoît<sup>1\*</sup>, ATEMBEH EFIETNGAB Noura<sup>2</sup>, FADANKA Stéphane<sup>3</sup>, BERINYUY-TATA Gloria<sup>3</sup>, FOMENA Abraham<sup>1</sup>**

<sup>1</sup>Laboratory of Parasitology and Ecology, Department of Animal Biology and Physiology, University of Yaounde I, Yaounde, Cameroon

<sup>2</sup>Centre for Research on Health and Priority Pathologies, Institute of Medical Research and Medicinal Plants Studies, PO box 13033 Yaoundé, Cameroon

<sup>3</sup>Mboalab Biotech, BP : 31066 Yaoundé, Cameroon

\* **Corresponding authors' email addresses** : [leguyzo@yahoo.fr](mailto:leguyzo@yahoo.fr)  
[amandineestellechoutezotiwa@gmail.com](mailto:amandineestellechoutezotiwa@gmail.com)

Volume 7, Issue 7, July 2025

Received : 15 May 2025

Accepted : 05 Jun 2025

Published : 09 July 2025

[Doi : 10.48047/AFJBS.7.7.2025.52-70](https://doi.org/10.48047/AFJBS.7.7.2025.52-70)

**Abstract Background:** The genus *Myxobolus* encompasses a diverse group of myxozoan parasites that represent significant threats to the health of freshwater fish populations, impacting both biodiversity and aquaculture productivity. These parasites are known to induce a range of pathological conditions, including gill infections, which can impair respiratory function in infected fish. Despite the increasing concern over myxozoan parasites, the diversity of *Myxobolus* species, particularly within African freshwater systems, remains poorly characterized.

**Methods:** Specimens of *Labeobarbus habereri* were collected from the Moliwè River, Cameroon. Parasitological examination included gross morphological assessment, histopathological analysis, and light microscopy to characterize the cysts and myxospores. Molecular identification was conducted through sequencing of the small subunit ribosomal DNA (SSU rDNA).

**Results:** Infected fish exhibited large, whitish cysts (1.9–2.5 mm in length, 60–1400 µm in width) located on the gill filaments. The mature myxospores were ovoid (8.7 ± 0.1 µm in length, 7.0 ± 0.08 µm in width), with two equal, apically oriented polar capsules measuring 4.4 (3.5–5.0) µm in length and 2.4 (1.8–3.1) µm in width. Molecular identification, based on SSU rDNA sequencing, confirmed *Myxobolus moliwensis* sp. nov. as novel species. Phylogenetic analysis positioned *M. moliwensis* sp. nov. within a sub-clade of gill-infecting *Myxobolus* species, showing a close phylogenetic relationship to *M. anaticus* and *M. tambroides*.

**Conclusion:** The identification of *Myxobolus moliwensis* sp. nov. significantly enhances our understanding of myxozoan diversity in African freshwater ecosystems. This study highlights the value of integrating both morphological and molecular approaches for accurate species identification and offers important contributions to the taxonomy of fish parasites, particularly within freshwater environments. **Keywords** : *Labeobarbus habereri* ; Myxosporea ; Fish parasites ; Morphological characterization ; SSU rDNA ; Histopathology ; Phylogenetic analysis

## 1. Introduction

Fish are crucial source of animal protein and provide essential nutrients that play a vital role in human nutrition (Fariya et al., 2022). The Cyprinidae family, with over 3,000 described species, is the most diverse group of freshwater fish (Imoto et al., 2013; Eschmeyer and Fong, 2015; Froese and Pauly, 2017; Tao et al., 2019). Certain species within this family, such as *Labeobarbus habereri* (Steindachner, 1912), are of significant economic importance in aquaculture, recreational fishing, and fisheries, serving as a critical protein source for humans (Skelton, 2001; Thai et al., 2007; Collins et al., 2012). The livelihoods of many people in Africa, particularly those in Moliwè and surrounding areas in Cameroon, a developing country, rely heavily on *L. habereri*. Disease outbreaks, however, represent a major threat to the economic viability of aquaculture (Bondad-Reantaso et al., 2005). These outbreaks can negatively affect the productivity of *L. habereri* in both natural and artificial aquatic systems, thereby jeopardizing the livelihoods of local communities that depend on this resource in Moliwè and its neighboring areas.

Myxozoa are a significant group of parasitic organisms that have considerable economic and nutritional implications due to their impact on both wild and cultured fish populations (Kent et al., 2001). The subphylum Myxozoa is a morphologically and genetically diverse group of microscopic parasites, comprising approximately 20% of all Cnidarian species (Atkinson et al., 2018). Their complex life cycle involves interactions with both vertebrates, primarily fish, and invertebrates such as annelid worms, in both marine and freshwater environments (Eszterbauer et al., 2015; Holzer et al., 2018). Myxozoans have been reported to infect almost every tissue and organ of fish, often showing some degree of tissue specificity (Mitchell, 1977; Lom and Dyková, 1992; Molnár, 1994).

Myxosporeans are traditionally identified based on the final developmental stage found in the vertebrate host: the myxospore (Lom and Dyková, 2006). To date, spore morphology has been the primary criterion for classifying the subphylum Myxozoa into its various classes, orders, families, and genera (Grasse, 1970; Lom and Arthur, 1989; Lom and Dyková, 1992). However, using morphological characteristics alone for species identification presents a challenge at the species level, as some myxospores are small and lack consistent, measurable traits. This limitation makes it difficult to make accurate taxonomic decisions based on morphology alone (Lom and Dyková, 2006). The advent of DNA sequencing has provided an additional, powerful tool for species identification (Fiala et al., 2015). Combining morphological and molecular characterization of myxosporeans aids in the development of a

comprehensive taxonomic database, which can be valuable for future studies on the ecology of these parasites. This approach is crucial for evaluating their impact on host populations and formulating appropriate management strategies.

In this study, we describe a new species of *Myxobolus* from Cameroon, based on an analysis of tissue tropism, myxospore morphology and dimensions, and SSU rDNA sequence data. This represents the first documentation of a Myxozoan species parasitizing *Labeobarbus habereri* and serves as an initial step towards a more comprehensive faunistic and taxonomic investigation of Myxozoa in the Southwest Region of Cameroon.

## **2. Materials and methods**

### **2.1. Fish collection**

Specimens of *Labeobarbus habereri* (Steindachner, 1914), were collected from the Moliwè River (4°03'669" N latitude; 9°14'736" E longitude), near Limbé, the capital of the Fako Division in the Southwest Region of Cameroon. Fish were captured using nets with a mesh size of 1 cm × 1 cm. After capture, the specimens were stored in coolers to maintain their integrity before being transported to the Parasitology and Ecology Laboratory at the University of Yaoundé I for further analysis. All fish collection protocols were approved by the ethical committee of the University of Yaoundé I.

### **2.2. Acquisition of morphological and histological data**

Upon arrival at the laboratory, fish were euthanized by immersion in an overdose of clove oil (Sigma-Aldrich, USA). Dissection of the gills revealed cysts on the filaments, indicating infection. Infection intensity was assessed using the gill cyst index as described by Kaur and Attri (2015). The average number of cysts on one side of the gill was determined and categorized as follows: light (1–5 cysts), moderate (6–10 cysts), heavy (11–20 cysts), or severe (21 or more cysts). Some cysts were ruptured between a slide and coverslip, and their contents were examined at 1000× magnification using a optic ivymen system microscope (Comecta-Ivymen, Spain) to identify myxospores. Other cysts were preserved in Eppendorf tubes containing 100% ethanol (Merck, Germany) for later analysis. Fresh spores were photographed and measured using an Amscope microscope (AmScope, USA) connected to a computer. Spore drawings were made using a Wild M-20 microscope (Wild Heerbrugg, Switzerland) equipped with a camera lucida. Myxospore identification was carried out according to the phenotypic characteristics outlined by Lom and Arthur (1989).

For histological analysis, gills with infested filaments were fixed in a 10% formalin solution (Sigma-Aldrich, USA) and embedded in molten paraffin (Sigma-Aldrich, USA). Tissue sections (4–8 µm) were obtained using a Reichert-Jung 2030 microtome (Reichert-Jung, Austria), stained with Hematoxylin and Eosin (Sigma-Aldrich, USA), and examined using the same optic microscope for morphological analysis.

### 2.3. Acquisition of molecular data

DNA was extracted from myxospores preserved in ethanol using the QIAGEN DNeasy Tissue and Blood Extraction Kit (Qiagen, Germany), following the manufacturer's protocol. The 18S ribosomal DNA (rDNA) gene was amplified with the following primers: MC5F (5'-CCTGAGAAACGGCTACCACATCCA-3') and MC3R (5'-GATTAGCCTGACAGATCACTCCACGA-3').

Polymerase chain reaction (PCR) was performed in a final volume of 20 µL, containing 7 µL of purified water, 10 µL of Master Mix (Thermo Fisher Scientific, USA), 1 µL of each primer, and 1 µL of DNA template. The PCR amplification profile was as follows: initial denaturation at 95°C for 5 minutes, followed by 35 cycles of denaturation at 95°C for 60 seconds, annealing at 60°C for 60 seconds, and elongation at 72°C for 120 seconds. A final elongation step was performed at 72°C for 5 minutes. Amplification efficiency was confirmed by electrophoresis of 5 µL of the PCR product on a 1.5% agarose gel stained with thiazole orange (Sigma-Aldrich, USA). The amplicons were purified using a QIAGEN PCR Clean-Up Kit (Qiagen, Germany) and sequenced at Inquaba Biotech (South Africa). The obtained sequences were visualized, assembled, and edited using BioEdit software (Hall, 1999), and ambiguous bases were resolved using the corresponding ABI chromatograms.

A total of 29 sequences of the 18S rDNA subunit from myxosporean species of the genus *Myxobolus* were selected for analysis. These sequences were obtained through a standard nucleotide-nucleotide BLAST (blastn) search on the National Center for Biotechnology Information (NCBI) website. Sequences from five recently described myxosporean species from Africa (Lekeufack-Folefack et al., 2019; Lekeufack-Folefack et al., 2021; Feudjio-Dongmo et al., 2022; Lekeufack-Folefack et al., 2022) were included. *Sphaerospora epinepheli* Supamattaya, Fischer-Scherl, Hoffman & Boonyaratpalin, 1991, was chosen as the outgroup. All sequences were aligned using BioEdit software (Hall, 1999).

## 2.4. Phylogenetic analyses

Bayesian inference and maximum likelihood methods were used to perform phylogenetic analyses. Bayesian inference was conducted using MrBayes software (Ronquist et al., 2012), with 1 million generations and a sampling frequency of 50. The average standard deviation of split frequencies was 0.001882 at the end of the analysis. The optimal evolutionary model was determined using jModelTest [28] based on the Akaike Information Criterion (AIC), with the GTR+I+G model being selected. Maximum likelihood estimates were obtained using IQ-TREE software (Nguyen et al., 2015), with 1000 bootstrap replicates. The phylogenetic trees were visualized using FigTree v1.3.1 (Rambaut, 2009) and edited in Adobe Illustrator (Adobe Systems, San Jose, USA).

## 3. Results

### 3.1. Taxonomic summary

Phylum: Cnidaria Hatschek, 1888

Subphylum: Myxozoa Grassé, 1970

Class: Myxosporidia Bütschli, 1881

Order: Bivalvulida Shulman, 1959

Suborder: Platysporina Kudo, 1919

Family: Myxobolidae Thélohan, 1892

Genus: *Myxobolus* Bütschli, 1882

Species: *Myxobolus moliwensis* sp. nov.

Type host: *Labeobarbus habereri* (Steindachner, 1914) (Cyprinidae)

Site of infection: gills

**Typical location:** Moliwè River, Limbe, Fako Division, South-west Region, Cameroon (Latitude: 4°03'669'' N, Longitude: 9°14'736'' E).

**Prevalence :** 23.3% (117 infected individuals out of 760 examined).

**Gill plasmodia index and infection intensity:** Mean  $\pm$  SD of  $8.37 \pm 1.18$ , corresponding to a moderate intensity of infection.

**Type material :** Formalin-fixed gills infected with cysts were preserved in 50 mL Eppendorf tubes and deposited in the parasitological collection of the Laboratory of Parasitology and Ecology, Faculty of Sciences, University of Yaoundé I, Cameroon (Catalogue Number: Myxo/2025/LPE-001). Additionally, a partial sequence of the small subunit ribosomal DNA (SSU rDNA, 882 bp) was deposited in GenBank under the accession number PV123175.

**Etymology:** The specific epithet is derived from the Moliwè River, the location where the host fish was captured.

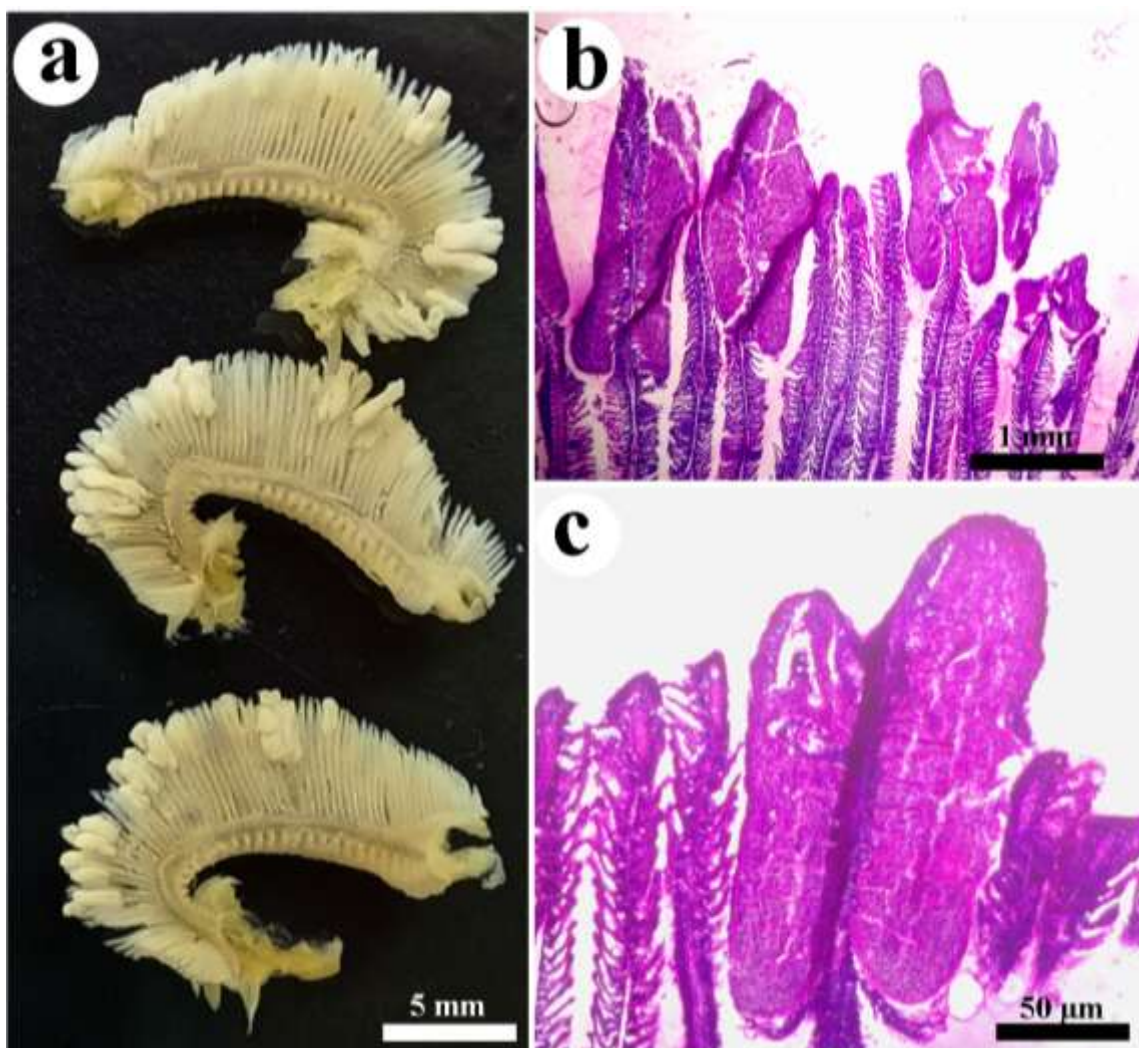


**Figure 1. Photomicrographs of the gills of *Labeobarbus habereri* showing cysts of *Myxobolus moliwensis* sp. nov. a:** Fresh preparation showing whitish cysts implanted on the apical parts of the gill filaments. **b:** Histological section of gill tissue stained with hematoxylin and eosin (H&E), illustrating cyst development on the gill filaments. **c:** Histological section stained with H&E, revealing cysts encompassing multiple gill lamellae and causing displacement of adjacent structures.

### 3.2. Vegetative stages

Large, whitish cysts of varying shapes and sizes were observed on the gills of *Labeobarbus habereri* (Figure 1a). These cysts primarily developed apically on the gill filaments but extended proximally to the base of the filaments in some cases (Figure 1a). The cysts measured between 1.9 and 2.5 mm in length and ranged from 60 to 1400  $\mu\text{m}$  in width. A maximum of 27 cysts were identified per parasitized fish, with both sides of the gills being equally affected. The development of these cysts was asynchronous (Figure 1a).

### 3.3. Histological examination

Histological analysis revealed that the large cysts associated with the parasite infecting *L. habereri* were polysporous and these cysts encompassed several gill lamellae, causing structural displacement and possibly impairing gill function (Figures 1b, c).

### 3.4. Morphology of myxospores

Mature myxospores were ovoid in shape. In the frontal view, the anterior pole appeared slightly narrowed and displayed an amorphous, homogeneous mass at its apex, while the posterior end was broad and rounded (Figures. 2a, b). In the sutural view, the myxospores exhibited a biconvex structure with thick, smooth valves. The suture line, which extended from the anterior to the posterior ends, was more pronounced in the posterior region (Figures. 2c, d). At the posterior pole, each valve possessed a distinct groove parallel and adjacent to the suture line, and the widest part of the spore was located at its mid-length. The myxospores contained two pyriformes polar capsules that were equal in size, apically oriented, and slightly converging anteriorly. These capsules occupied the anterior half of the spore cavity and each contained 4–6 coils of the polar tubule arranged obliquely to the long axis of the capsule (Figure. 2f). No intercapsular appendix was present. The posterior half of the spore cavity was filled with a finely granular, homogeneous mass of sporoplasm. This sporoplasm extended slightly into the intercapsular space, forming a seamless transition between the anterior and posterior regions of the spore cavity.

### Remarks:

The parasite species collected from the gills of *Labeobarbus habereri* closely resembles several myxobolid species reported globally, particularly in terms of size and morphology. These include *Myxobolus branchilateralis* Molnár, Eszterbauer, Marton, Székely & Eiras, 2012, found at the base of gill filaments of *Barbus barbus* (Linnaeus, 1758)

in Hungary; *M. opsaridiumi* Lekeufack-Folefack, Tchoutezo-Tiwa, Al-Tamimi, Fomena, Al-Omar & Mansour, 2021, parasitizing the skin, muscles, and spleen of *Opsaridium ubangiense* Pellegrin, 1901 in Cameroon; *M. tambroides* Székely, Shaharom, Cech, Mohamed, Zin, Borkhanuddin, Ostoros & Molnár, 2012, identified on the gill lamellae of *Tor tambroides* (Bleeker, 1854) in Malaysia; *M. lalbaghensis* Banerjee Bandyopadhyay, Göçmen & Mitra, 2011, isolated from the gills of *Labeo bata* (Hamilton, 1822) in India; *M. calcariferum* Basu & Halder, 2003, found within the gill lamellae of *Lates calcarifer* (Bloch, 1790) in India; *M. anatolicus* Pekmezci, 2014, from the gills of *Capoeta tinca* (Heckel, 1843) in Turkey; *M. eirasianus* Cech, Molnár & Székely, 2012, located on the gills of *Blicca bjoerkna* (Linnaeus, 1758) in Hungary; and *M. goreensis* Fall, Kpatcha, Diebakate, Faye & Toguebaye, 1997, found in the gill filaments of *Mugil cephalus* (Linnaeus, 1758) in Senegal (Table 1). Notably, *M. branchilateralis*, collected from young *Barbus barbuis* in the Danube River, forms spores averaging  $9.7 \mu\text{m} \times 8.2 \mu\text{m}$ , with larger polar capsules ( $5.6 \mu\text{m} \times 3 \mu\text{m}$ ) and a thin mucous envelope, features that differentiate it from the current species, whose spores measure  $8.7 \mu\text{m} \times 7.0 \mu\text{m}$  on average. Similarly, *M. opsaridiumi* exhibits more developed ovoid spores ( $10.7 \mu\text{m} \times 9 \mu\text{m}$ ) and polar tubules with 5–7 coils perpendicular to the polar capsule axis. *Myxobolus tambroides* produces longer spores ( $9.9 \mu\text{m}$  vs.  $8.7 \mu\text{m}$  on average) and larger pear-shaped polar capsules ( $5.7 \mu\text{m}$  vs.  $4.4 \mu\text{m}$  on average), with knob-like structures between capsule bases. *Myxobolus lalbaghensis* forms blunt-ended spores and pear-shaped polar capsules with an anterior tip. While *M. calcariferum* spores are almost spherical ( $6.6 \mu\text{m} \times 6.2 \mu\text{m}$  on average), and *M. anatolicus* spores are significantly elongated ( $10.1 \mu\text{m}$  on average), both differ from the species under study. The resemblance to *M. eirasianus* is weak due to the pyriform shape and larger dimensions of the latter's spores ( $12.8 \mu\text{m} \times 9.6 \mu\text{m}$ ) and polar capsules ( $5.9 \mu\text{m} \times 3.5 \mu\text{m}$ ). Lastly, *M. goreensis* spores ( $10 \mu\text{m}$  on average) are larger and have pyriform polar capsules with perfectly round anterior openings, contrasting the bluntly pointed anterior ends of the presently described species.

### 3.5. Molecular characterization

A partial sequence of the 18S ribosomal RNA gene (rDNA), comprising 882 base pairs, was successfully amplified and sequenced. The sequence exhibited a GC content of 45.9%. Comparative analysis using the BLASTn tool demonstrated that this sequence is novel and distinct from all known myxosporean sequences available in public genomic databases.

The highest sequence similarities were observed with *Myxobolus tambroides* (95.59%) and *Myxobolus anatolicus* (94.79%).

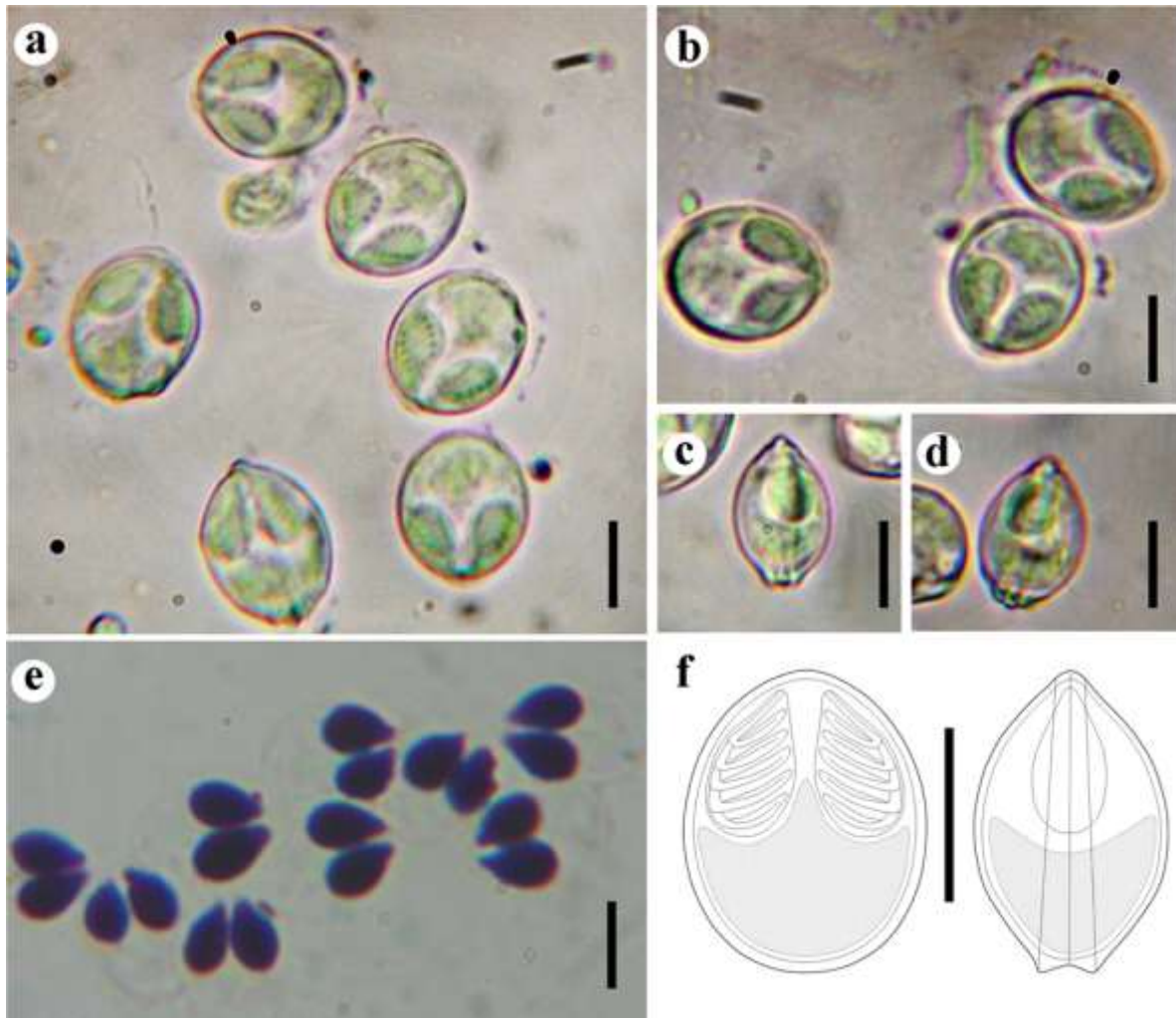


**Figure 2.** Photomicrographs and illustrations of mature myxospores of *Myxobolus moliwensis* sp. nov. a – b: Myxospores in frontal view. c – d: Myxospores in lateral view. e: Myxospores stained with May-Grünwald-Giemsa highlighting structural details. f: Diagrammatic representation of the myxospore of *Myxobolus moliwensis* sp. nov. in frontal and lateral views. Scale bars: 5  $\mu$ m.

### 3.6. Phylogenetic analyses

Phylogenetic analyses based on SSU rDNA sequences, including the newly obtained in this study, consistently yielded robust topologies using both Maximum Likelihood (ML) and Bayesian Inference (BI) methods (Fig. 3). The resulting phylogenetic tree classified the parasite species into two primary clades (Fig. 3). Clade A contains species that parasitize the fins, skin, spleen, and scales of African Cypriniformes within the family Cyprinidae, while Clade B encompasses species that infect the gills, oral cavity, intestines, and muscles of Cypriniformes (Cyprinidae) from Europe, America, and Asia. The parasite species identified

on the gills of *Labeobarbus habereri* is positioned within Clade B, specifically within a subclade comprising gill-parasitizing species of Cyprinidae. This species forms a distinct subclade with *Myxobolus anaticus* and *Myxobolus tambroides*, which infect *Coptodon tinca* and *Tor tambroides*, respectively. Importantly, the grouping of these species is not influenced by their geographical distribution but is instead driven by shared morphological and genetic characteristics, underscoring the relevance of these factors in their evolutionary relationships.

#### 4. Discussion

Myxosporeans represent a highly diverse group of parasitic organisms, with taxonomy historically reliant on the morphological features of the myxospore (Fiala et al., 2015). However, significant morphological similarities among species have often complicated accurate identification (Liu et al., 2013). To address this challenge, a holistic approach that integrates spore morphology, tissue tropism, host specificity, and molecular data has been recommended (Cech et al., 2012; Atkinson et al., 2015). This integrated methodology was applied in the present study to characterize a histozoic myxosporean species isolated from the gills of *Labeo habereri*. The phenotypic and molecular analyses indicate that this parasite species does not match any previously described species. Consequently, we propose this novel parasite as a new species, designated *Myxobolus moliwensis* sp. nov. The specific epithet, "moliwensis," honors the Moliwe River, where the host fish was collected.

The cysts of *M. moliwensis* sp. nov. were observed at the tips of the gill filaments, where they caused engulfment of the gill lamellae. This process resulted in the destruction of these structures and significant gill deformation, potentially impairing their physiological functions. The gills, as critical respiratory organs, play a central role in oxygen exchange, and their dysfunction can lead to reduced gas exchange efficiency and heightened susceptibility to environmental stressors. Our findings align with Dyková and Lom (1978), who reported that myxosporean infections on gills often induce epithelial hyperplasia, leading to tissue destruction and lamellar deformation. Similarly, Oğuz and Oğuz (2019) noted that vegetative stages of myxosporeans can disrupt gill architecture, causing lamellar fusion as a defense mechanism. While this fusion provides a protective barrier, it reduces the respiratory surface area, exacerbating the physiological impact on the host.

**Table 1. Comparative chart between *Myxobolus moliwensis* sp. nov. (in bold) with morphologically similar species (Mean values of spore dimensions are given in  $\mu\text{m}$  and range in parentheses)**

| <i>Myxobolus</i> spp.         | Spore measurement         |                              |                               | Polar capsule measurement    |                              | Relative length of the polar capsules | Number of coils of polar filament | Infestation site      | Host species                 | Country  | Genbank Accession number | Reference                               |
|-------------------------------|---------------------------|------------------------------|-------------------------------|------------------------------|------------------------------|---------------------------------------|-----------------------------------|-----------------------|------------------------------|----------|--------------------------|-----------------------------------------|
|                               | Length                    | Width                        | Thickness                     | Length                       | Width                        |                                       |                                   |                       |                              |          |                          |                                         |
| <i>M. moliwensis</i> sp. nov. | <b>8.7±0.1</b><br>(8-9.7) | <b>7.0±0.08</b><br>(6.6-8.1) | <b>5.8±0.2</b><br>(5.6 – 6.2) | <b>4.4±0.06</b><br>(3.5-5.0) | <b>2.4±0.05</b><br>(1.8-3.1) | =                                     | 4-5                               | Gills                 | <i>Labeobarbus habereri</i>  | Cameroon | PV123175                 | Present study                           |
| <i>M. branchilateralis</i>    | 9.7 ± 0.4<br>(9.4-10.4)   | 8.2 ± 0.6<br>(7.5-9.1)       | 6.4 ± 0.7<br>(5.2-7.2)        | 5.6± 0.4<br>(5.3-6.8)        | 3 ± 0.3<br>(2.5-3.3)         | =                                     | 6                                 | Gills                 | <i>Barbus barbus</i>         | Hungary  | JQ388888                 | Molnár <i>et al.</i> , 2012             |
| <i>M. opsaridiumi</i>         | 10.7<br>(10-11.5)         | 9 (8-10)                     | 6.2<br>(5.6-7.2)              | 5 (4.3-6)                    | 2.7<br>(2.2-3)               | =                                     | 5-7                               | Skin, spleen muscles, | <i>Opsaridium ubangiense</i> | Cameroon | MN497413                 | Lekeufack-Folefack <i>et al.</i> , 2021 |
| <i>M. tambroides</i>          | 9.9± 0.43<br>(8.8-10.6)   | 7.4±0.24<br>(6.8-7.9)        | 7.2±0.38<br>(7-7.9)           | 5.7±0.7<br>(5-7)             | 2.6±0.1<br>(2.4-2.9)         | =                                     | 5-6                               | Gills                 | <i>Tor tambroides</i>        | Malaysia | JX028236                 | Székely <i>et al.</i> , 2012            |
| <i>M. lalbaghensis</i>        | 9.2 ± 1.0<br>(7.6- 11.9)  | 6.8 ± 1.1<br>(5.1-8.5)       | /                             | 5.1 ± 0.7<br>(4.2-6.8)       | 2.3 ± 0.3<br>(1.7- 2.5)      | =                                     | 4-5                               | Gills                 | <i>Labeo bata</i>            | India    | /                        | Banerjee <i>et al.</i> , 2011           |
| <i>M. calcariferum</i>        | 6.6 ± 0.3<br>(6.1-7.1)    | 6.2 ± 0.2<br>(5.7-6.5)       | /                             | 4.2 ± 0.2<br>(3.8-4.5)       | 2.3 ± 0.2<br>(2.0-2.7)       | =                                     | 4-5                               | Gills                 | <i>Lates calcarifer</i>      | India    | /                        | Basu & Halder, 2003                     |
| <i>M. anatolicus</i>          | 10.1 ± 0.4<br>(9.4 -10.7) | 6.9 ± 0.2<br>(6.6 - 7.2)     | 4.5 ±0.36<br>(4.4 -4.6)       | 4.6 ± 0.4<br>(4.4 - 4.8)     | 2.1 ± 0.1<br>(2 - 2.3)       | =                                     | 5-6                               | Gills                 | <i>Copoeta tinca</i>         | Turkey   | KF537629                 | Pekmezci 2014                           |
| <i>M. eirasiiianus</i>        | 12.8 ± 0.3<br>(12.6-13.5) | 9.6 ± 0.42<br>(9-10.3)       | 7.9 ± 0.5<br>(7.2- 9)         | 5.9 ± 0.28<br>(5.4-6.3)      | 3.5 ± 0.1<br>(3.2-3.7)       | =                                     | 6                                 | Gills                 | <i>Blicca bjoerkna</i>       | Hungary  | JF311900                 | Cech <i>et al.</i> , 2012               |
| <i>M. goreensis</i>           | /                         | 10.9±0.68<br>(10-13)         | /                             | 4.1±0.4<br>(4-5)             | 3.0±0.2<br>(2-4)             | =                                     | 6                                 | Gills                 | <i>Mugil cephalus</i>        | Senegal  | /                        | Fall <i>et al.</i> , 1997               |

The arithmetic means of the measured variables are followed in brackets by the minimum and maximum values

/ : No data available ; = : equal

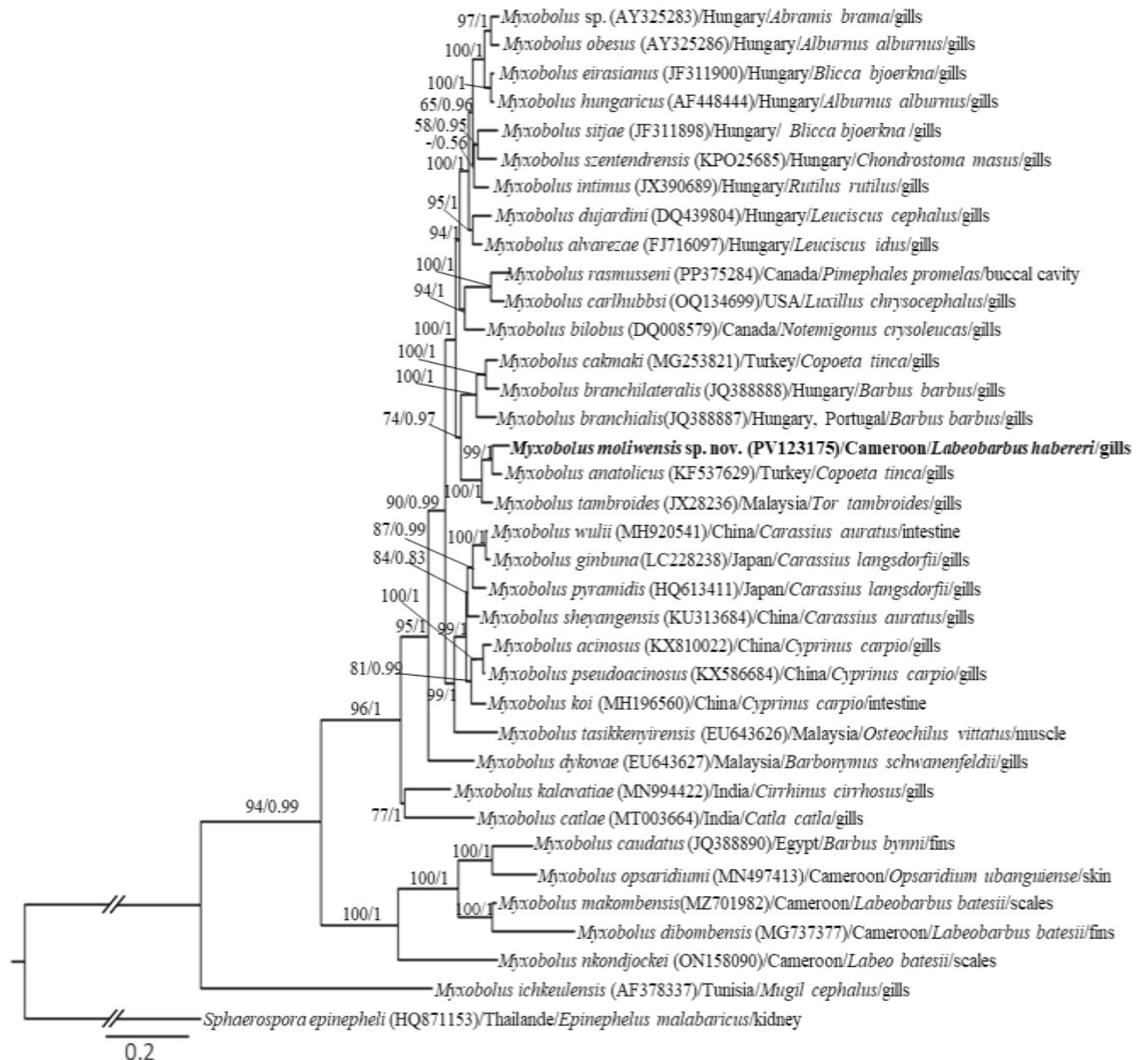


**Figure 3.** Phylogenetic tree based on Bayesian inference and maximum likelihood methods of the SSU rDNA of *Myxobolus* species related to *Myxobolus moliwensis* sp. nov. (indicated in bold). Species names are accompanied by their corresponding GenBank accession numbers in bracket, locality, host species, and parasitized organ. The numbers on the branch nodes represent posterior probability/bootstrap support; dashes indicate bootstrap values below 50. *Sphaerospora epinepheli* was used as outgroup. The double slash (//) symbolizes artificial shortening of the branches for visualisation

The gill cysts index in this study revealed a moderate infection intensity caused by *M. moliwensis* sp. nov., suggesting that while the infection does not reach critical levels, it has notable implications for host health. Moderate infections of similar nature have been reported, by Kaur and Attri (2015) in *Henneguya bicaudi* infections of *Cirrhinus mrigala* in India, highlighting the global prevalence of such parasitic impacts on fish populations.

Phylogenetic analyses positioned *M. moliwensis* sp. nov. within Clade B, forming a subclade with *Myxobolus anaticus* and *Myxobolus tambroides*, both of which parasitize species within the Cyprinidae family. This subclade is characterized by oval-shaped spores, a feature shared by the three species and reinforcing their phylogenetic affinity. Previous studies (Liu et al., 2019; Abdel-Gaber et al., 2017) have similarly demonstrated a correlation between spore morphology and phylogenetic relationships. Interestingly, the subclade of oval-spored *Myxobolus* species is phylogenetically linked to another clade of gill parasites infecting Cyprinidae in Turkey and Malaysia. This observation supports findings by Shin et al. (2014) and Abdel-Gaber et al. (2017), who proposed that Myxobolidae phylogeny is strongly influenced by tissue tropism, resulting in clusters of species with highly specific host-site affinities. Additionally, the grouping of Cypriniform parasites within Clade B emphasizes the phylogenetic significance of host order and family, corroborating previous research by Rocha et al. (2019) and Vieira et al. (2024).

## 5. Conclusion

This study highlights the significance of employing integrated, multidimensional approaches to the classification of myxosporeans, encompassing both morphological and genetic analyses. A comprehensive understanding of myxosporean diversity is vital for elucidating the evolutionary dynamics of these parasites and their intricate interactions with aquatic hosts. Such insights into host-parasite relationships are critical for devising effective management and conservation strategies for impacted fish species, ultimately supporting the preservation of aquatic biodiversity.

**Conflicts of interest :** The authors declare no conflicts of interest regarding the publication of this paper.

**Acknowledgements :** The authors express their gratitude to the Faculty of Science at the University of Yaoundé I and Mboalab Biotech Yaoundé–Cameroon for providing the necessary facilities to complete this work.

## 6. References

- Abdel-Gaber, R., Abdel-Ghaffar, F., Maher, S., El-Mallah, A.M., Al Quraishy, S. and Mehlhorn, H. (2017). Morphological re-description and phylogenetic relationship of five myxosporean species of the family Myxobolidae infecting Nile tilapia. *Dis. Aquat. Organ*, 124(3), 201-214. <https://doi.org/10.3354/dao03118>
- Atkinson, S.D., Bartosova-Sojkova, P., Whipps, C.M. and Bartholomew, J.L. (2015). Approaches for characterizing myxozoan species. In Okamura et al., (Eds.), *Myxozoan Evolution, Ecology and Development* (pp. 111–123). Springer Cham. [https://doi.org/10.1007/978-3-319-14753-6\\_6](https://doi.org/10.1007/978-3-319-14753-6_6)
- Atkinson, S.D. ; Bartholomew, J.L. and Lotan T. (2018) Myxozoans: Ancient metazoan parasites find a home in phylum Cnidaria. *Zoology*, 129, 66-68. <https://doi.org/10.1016/j.zool.2018.06.005>
- Bondad-Reantaso, M.G., Subasinghe, R.P., Arthur, J.R., Ogawa, K., Chinabut, S., Adlard, R., Tan, Z. and Shariff, M. (2005). Disease and health management in Asian aquaculture. *Vet. Parasitol*, 132(3-4), 249-272. <https://doi.org/10.1016/j.vetpar.2005.07.005>
- Cech, G., Molnár, K. and Székely, Cs. (2012). Molecular genetic studies on morphologically indistinguishable *Myxobolus* spp. infecting cyprinid fishes, with the description of three new species, *M. alvarezae* sp. nov., *M. sitjae* sp. nov. and *M. eirasianus* sp. nov. *Acta Parasitol*, 57(4), 354–366. <https://doi.org/10.2478/s11686-012-0045-2>
- Collins, R.A., Armstrong, K.F., Meier, R., Yi, Y., Brown, S.D., Cruickshank, R.H., Keeling, S. and Johnston, C. (2012). Barcoding and border biosecurity: identifying cyprinid fishes in the aquarium trade. *PloS one*, 7(1), e28381. <https://doi.org/10.1371/journal.pone.0028381>
- Csaba, G. (1976). An unidentifiable extracellular sporozoan parasite from the blood of the carp. *Parasitol. Hung*, 9, 21-24.
- Dariba, D., Taboada, G.L., Doallo, R. and Posada, D. (2012). jModeltest 2: more models, new heuristics and parallel computing. *Nat. Methods*, 9 : 772. <https://doi.org/10.1038/nmeth.2109>
- Eichlin, T.C. and Cunningham, H.B. (1978). The Plusiinae (Lepidoptera: Noctuidae) of America North of Mexico, emphasizing genitalic and larval morphology. *USDA Tech. Bull*, 1567, 122.

Dyková, I., and Lom, J. (1978). Histopathological changes in fish gills infected with myxosporidian parasites of the genus *Henneguya*. *J. Fish Biol*, 12(3), 197-202. <https://doi.org/10.1111/j.1095-8649.1978.tb04165.x>

Eschmeyer, W.N. and Fong, J.D. 2015. Species by family/subfamily in the catalog of fishes. <http://researcharchive.calacademy.org/research/ichthyology/catalog/speciesbyfamily>.

Eszterbauer, E., Atkinson, S., Diamant, A., Morris, D., El-Matbouli, M. and Hartikainen, H. (2015). Myxozoan Life Cycles: Practical Approaches and Insights. In Okamura et al., (Eds.), *Myxozoan Evolution, Ecology and Development* (pp. 174 – 198). Springer Cham. [https://doi.org/10.1007/978-3-319-14753-6\\_10](https://doi.org/10.1007/978-3-319-14753-6_10)

Fariya, N., Kaur, H., Singh, M., Abidi, R., El-Matbouli, M. and Kumar, G. (2022). Morphological and Molecular Characterization of a New Myxozoan, *Myxobolus grassi* sp. nov. (Myxosporea), Infecting the Grass Carp, *Ctenopharyngodon idella* in the Gomti River, India. *Pathogens*, 11, 303. <https://doi.org/10.3390/pathogens11030303>

Feudjio-Dongmo, B., Lekeufack-Folefack, G.B., Tene-Fossog, B., Fomena, A., Wondji, C.S., Yurakhno, V.M., Alomar, S. and Mansour, L. (2022). *Myxobolus makombensis* n. sp. infection in African carp *Labeobarbus batesii* from the Makombè River, Cameroon: morphological and molecular characterization. *Dis. Aquat. Organ*, 151, 75-84. <https://doi.org/10.3354/dao03691>

Fiala, I., Bartošova-Sojková, P., Okamura B, and Hartikainen, H. (2015) Adaptive radiation and evolution within the Myxozoa. In Okamura et al., (Eds.), *Myxozoan Evolution, Ecology and Development* (pp. 69–84). Springer Cham. [https://doi.org/10.1007/978-3-319-14753-6\\_4](https://doi.org/10.1007/978-3-319-14753-6_4)

Froese, R. and Pauly, D. (2017) Fish Base. World Wide Web Electronic Publication. [www.fishbase.org](http://www.fishbase.org)

Grassé, P.P. (1970). Embranchement des myxozoaires. In Précis de zoologie 1, Invertébrés, 2nd ed., Grassé P. P., Poisson R. A. and Tuzet O. (eds). Masson et Cie, Paris, France, 107-112.

Hall, T. (1999). BioEdit: a user-friendly biological sequence alignment editor and analysis program for Windows 95/98/ NT. *Nucleic Acids Symp. Ser*, 41 : 95–98.

Holzer, A.S., Bartošová-Sojková, P., Born-Torrijos, A., Lövy, A., Hartigan, A. and Fiala, I. (2018). The joint evolution of the Myxozoa and their alternate hosts: A cnidarian recipe for success and vast biodiversity. *Mol. Ecol*, 27, 1651–1666. <https://doi.org/10.1111/mec.14558>

Imoto, J.M., Saitoh, K., Sasaki T., Yonezawa, T., Adachi, J., Kartavtsev, Y.P., Miya, M., Nishida, M. and Hanzawa, N. (2013). Phylogeny and biogeography of highly diverged freshwater fish species (Leuciscinae, Cyprinidae, Teleostei) inferred from mitochondrial genome analysis. *Gene*, 514(2), 112-124. <https://doi.org/10.1016/j.gene.2012.10.019>

Kaur, H., and Attri, R. (2015). Morphological and molecular characterization of *Henneguya bicaudi* n. sp. (Myxosporea: Myxobolidae) infecting gills of *Cirrhinus mrigala* (Ham.) in Harike Wetland, Punjab (India). *Parasitol. Res*, 114, 4161-4167. <https://doi.org/10.1007/s00436-015-4647-0>

Kent, M., Andree, K., Bartholomew, K., El-Matbouli, Desser, S., Delving, R., Feist, S., Hedrick, R., Hoffman, R., Khattra, J., Hallet, S., Lester, J., Longshaw, M., Palenzuela, O., Sidal, M. and Xiao, C. 2001: Recent advances in our knowledge of the Myxozoa. *J. Eukaryot. Microbiol*, 49(4), 395-413. <https://doi.org/10.1111/j.1550-7408.2001.tb00173.x>

Lekeufack Folefack, G.B., Abdel-Baki, A.A.S., Ateba, N.O.O., Fomena, A., and Mansour, L. (2019). Morphological and molecular characterization of *Myxobolus dibombensis* sp. n. (Myxozoa: Myxobolidae), a parasite of the African carp *Labeobarbus batesii* (Teleostei: Cyprinidae) from Dibombe River, Cameroon. *Parasitol. Res*, 118, 763-771. <https://doi.org/10.1007/s00436-019-06209-w>

Lekeufack-Folefack, G.B., Tchoutezo-Tiwa, A.E., Al-Tamimi, J., Fomena, A., Al-Omar, S.Y., and Mansour, L. (2021). *Myxobolus opsaridiumi* sp. nov. (Cnidaria: Myxosporea) infecting different tissues of an ornamental fish, *Opsaridium ubangiensis* (Pellegrin, 1901), in Cameroon: morphological and molecular characterization. *Eur. J. Taxon*, 733, 56-71. <https://doi.org/10.5852/ejt.2021.733.1221>

Lekeufack-Folefack, G.B., Feudjio-Dongmo, B., Tene-Fossog, B., Fomena, A., Wondji, C.S., Al-Tamimi, J. and Mansour, L. (2022). Morphological and Molecular characterization of *Myxobolus nkondjockei* sp. nov. (myxozoa: Myxobolidae), a parasite of *Labeo batesii* Boulenger, 1911 (Teleostei: Cyprinidae) from Makombè river in Cameroon. *Acta Parasitol*, 67(4), 1573-1583. <https://doi.org/10.1007/s11686-022-00609-2>

- Liu, Y., Whipps, C.M., Gu, Z.M., Huang, M.J., He, L.Y. and Molnár K. (2013). *Myxobolus musseliusae* (Myxozoa: Myxobolidae) from the gills of common carp *Cyprinus carpio* and revision of *Myxobolus dispar* recorded in China. *Parasitol. Res*, 112: 289–296. <https://doi.org/10.1007/s00436-012-3136-y>
- Liu, X.H., Zhang, D.D., Yang, C.Z. and Zhao, Y.J. (2019). Morphological and molecular identification of *Myxobolus parakoi* sp. nov (Myxozoa: Myxobolidae), from *Cyprinus carpio* in Chongqing China. *Zootaxa*, 4657(1), 117-126. <https://doi.org/10.11646/zootaxa.4657.1.4>
- Lom, J. and Arthur, J.R. (1989). A guideline for the preparation of species descriptions in Myxosporea. *J. Fish Dis*, 12(2), 151-156. <https://doi.org/10.1111/j.1365-2761.1989.tb00287.x>
- Lom, J. and Dyková, I. 1992: Protozoan parasites of fishes. In Elsevier Amsterdam-London-New York-Tokyo (Eds.), *Developments in aquaculture and fisheries science*, 26. Elsevier Science Publishers, 159-235.
- Lom, J. and Dyková, I. 2006: Myxozoan genera: definition and notes on taxonomy, life-cycle terminology and pathogenic species. *Folia Parasitol*, 53: 1-36. <https://doi.org/10.14411/fp.2006.001>
- Mitchell, L.G. (1977). Myxosporidla. In: Krier, J.P. (ed.) *Parasitic protozoa*. Vol. IV. Academic Press, New York, p. 115-154
- Molnár, K. (1994). Comments on the host, organ and tissue specificity of fish myxosporeans and on the types of their intrapiscine development. *Parasitol. Hung*, 27, 5-20.
- Molnár, K., and Eszterbauer, E. (2015). Specificity of infection sites in vertebrate hosts. In Okamura et al., (Eds.), *Myxozoan Evolution, Ecology and Development* (pp. 295–313). Springer Cham. [https://doi.org/10.1007/978-3-319-14753-6\\_16](https://doi.org/10.1007/978-3-319-14753-6_16)
- Nguyen, L.T., Schmidt, H.A., Von Haeseler, A., and Minh, B.Q. (2015). IQ-TREE: a fast and effective stochastic algorithm for estimating maximum-likelihood phylogenies. *Mol. Biol. Evol*, 32(1), 268-274. <https://doi.org/10.1093/molbev/msu300>
- Oğuz, A.R. and Oğuz, E.K. (2019). Histopathology and immunohistochemistry of gills of Van fish (*Alburnus tarichi* Gildenstädt, 1814) infected with myxosporean parasites. *J. Histotechnol*, 43(2), 76-82 <https://doi.org/10.1080/01478885.2019.1686848>

Rambaut, A. (2009). FigTree v1. 3.1 : Tree figure drawing tool. <http://tree.bio.ed.ac.uk/software/figtree/>.

Rocha, S., Azevedo, C., Oliveira, E., Alves, A., Antunes, C., Rodrigues, P. and Casal, G. (2019). Phylogeny and comprehensive revision of mugiliform-infecting myxobolids (Myxozoa, Myxobolidae), with the morphological and molecular redescription of the cryptic species *Myxobolus exiguus*. *Parasitol*, 146, 479–496. <https://doi.org/10.1017/S0031182018001671>

Ronquist, F., Teslenko, M., Van Der Mark, P., Ayres, D.L., Darling, A., Höhna, S., Larget, B., Liu, L., Suchard, M.A. and Huelsenbeck, J.P. (2012). MrBayes 3.2: efficient Bayesian phylogenetic inference and model choice across a large model space. *Syst. Biol*, 61(3), 539-542. <https://doi.org/10.1093/sysbio/sys029>

Shin, S.P., Jeong, J.M., Jun, J.W., Kim, J.H., Han, J.E., Baek, G.W., and Park, S.C. (2014). The phylogenetic study on *Thelohanellus* species (Myxosporea) in relation to host specificity and infection site tropism. *Mol. Phylogenet. Evol*, 72, 31-34. <https://doi.org/10.1016/j.ympev.2014.01.002>

Skelton, C.E. (2001). New dace of the genus *Phoxinus* (Cyprinidae: Cypriniformes) from the Tennessee River drainage, Tennessee. *Copeia*, 1, 118-128. [https://doi.org/10.1643/0045-8511\(2001\)001\[0118:NDOTGP\]2.0.CO;2](https://doi.org/10.1643/0045-8511(2001)001[0118:NDOTGP]2.0.CO;2)

Tao, W., Yang, L., Mayden, R.L. and He, S. (2019). Phylogenetic relationships of Cypriniformes and plasticity of pharyngeal teeth in the adaptive radiation of cyprinids. *Sci. China Life Sci*, 62, 553-565. <https://doi.org/10.1007/s11427-019-9480-3>

Thai, B.T., Phan, P.D. and Austin, C.M. (2007). Phylogenetic evaluation of subfamily classification of the Cyprinidae focusing on Vietnamese species. *Aquat. Living Resour*, 20(2), 143-153. <https://doi.org/10.1051/alr:2007025>

Vieira, D.H.M.D., Osaki-Pereira, M.M., Abdallah, V.D., Oliveira, S.L.P., Duarte, A.G.T., da Silva, R.J. and de Azevedo, R.K. (2024). Morphological and Molecular Analysis Describing Two New Species of *Myxobolus* (Cnidaria, Myxosporea) in *Mugil curema* (Mugilidae) from Brazil. *Taxonomy*, 4(3), 548-560. <https://doi.org/10.3390/taxonomy4030026>